Do gravity data justify a rifted „Liguro-Provençial Basin“? – A few thoughts on gravity data analysis

Hajo Götze (CAU), Ronja Strehlau (CAU), Anke Dannowski (GEOMAR), Magdalena Scheck-Wenderoth (GFZ, RWTH Aachen), Denis Anikiev (GFZ), Sabine Schmidt (CAU) & Christian Plonka (GFZ)

Content:

- Data basis
- Methods used
- Interpretation & results

Projects funded by Deutsche Forschungsgemeinschaft (DFG):
Go 380/36-1, SCHE 674/7-1 and SCHE 674/8-1 (SPP 2017 – MB 4D)

Datebase

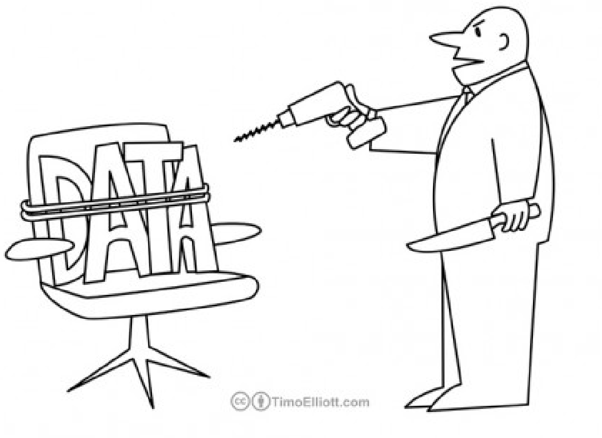

"If you don't reveal some insights soon, I'm going to be forced to slice, dice, and drill!"

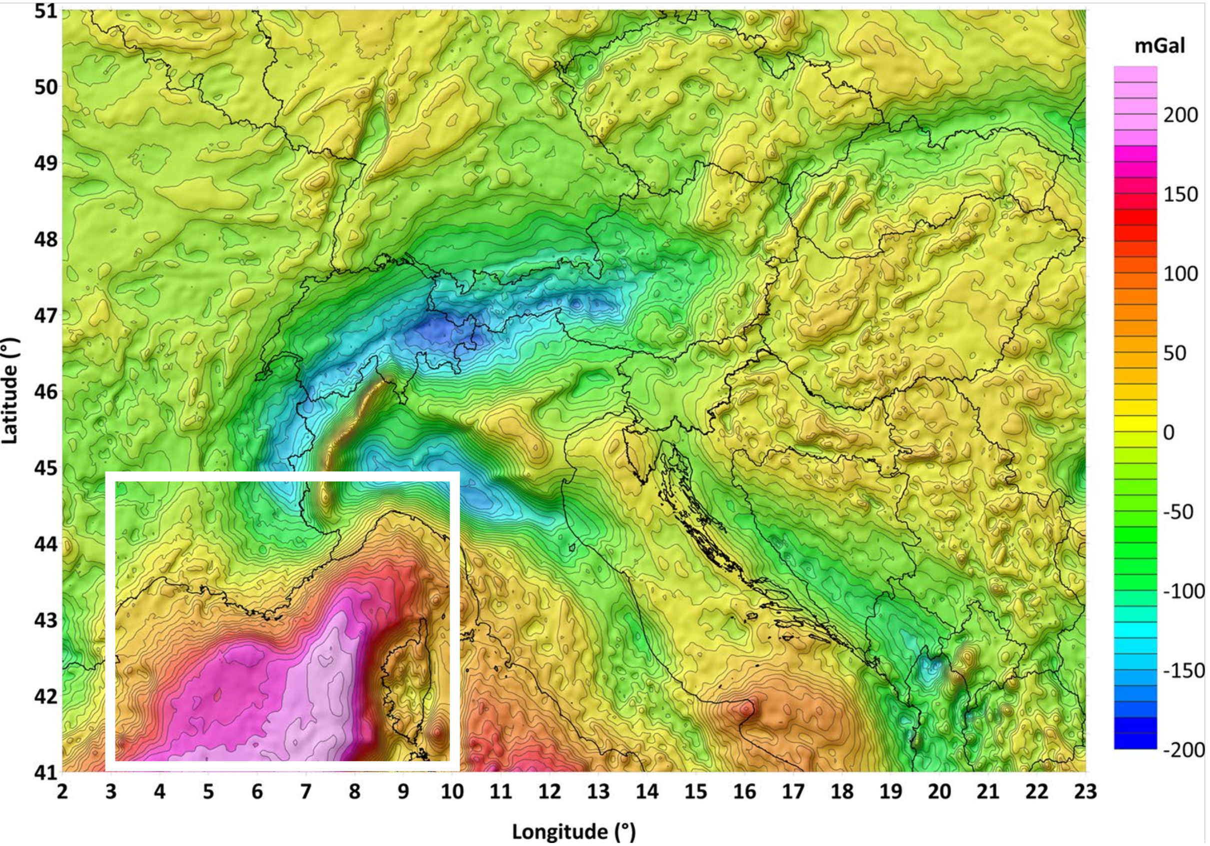

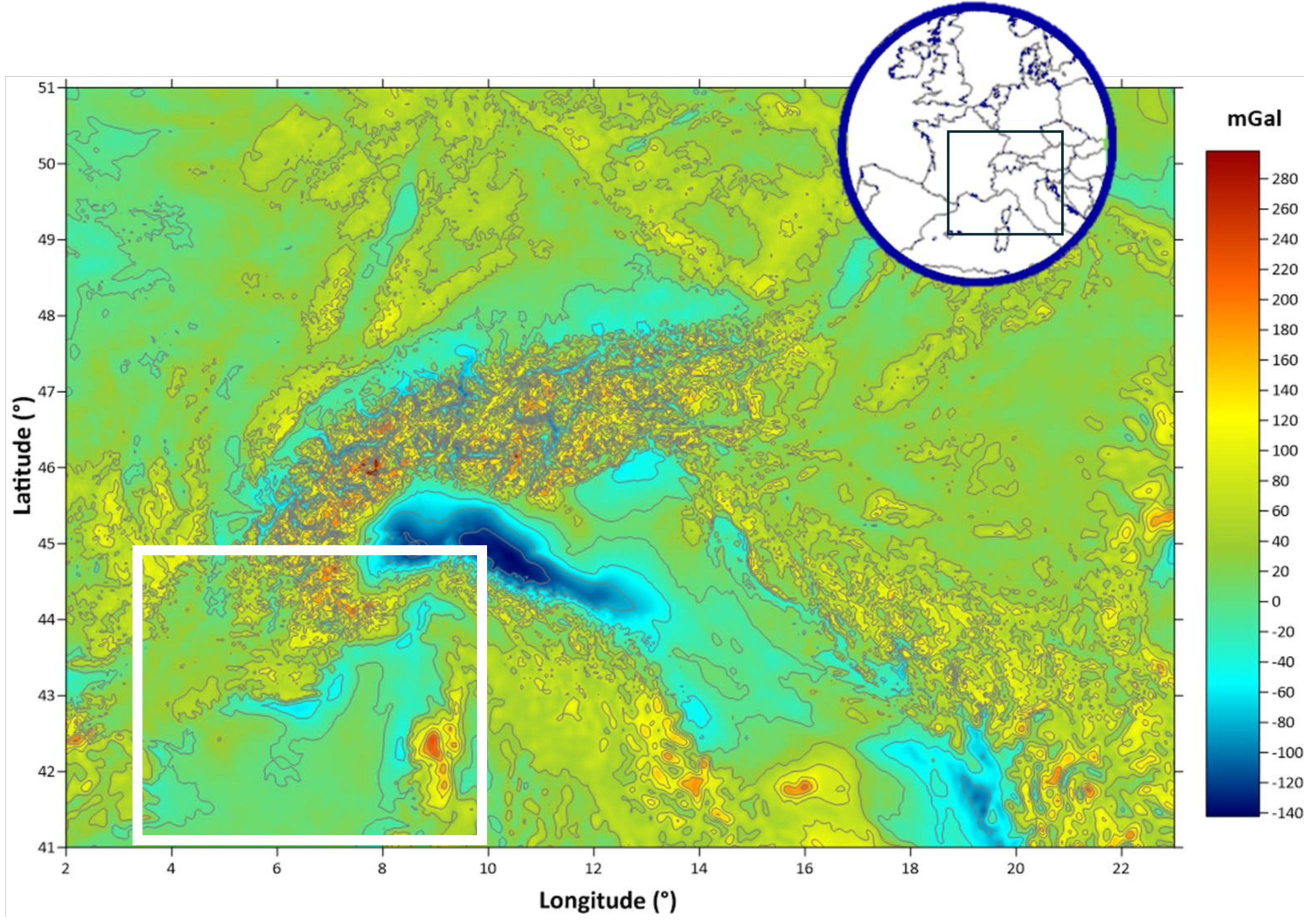

With the publication of the new gravity field compilations by the "AlpArray Gravity Research Group, AAGRG" (Zahorec et al., 2021), a database is now available that meets the requirements for the 3D modeling. The newly computed gravity fields are published on a 4 km x 4 km grid (Zahorec et al., 2021) for both completed Bouguer- (left) and Free air anomalies (right). These compilations are determined by the negative gravity in the Alps and the Po Basin in northern Italy, the Ivrea high in the western Italian Alps and the dominant high in the Bouguer anomaly in the Liguro-Provençal basin.

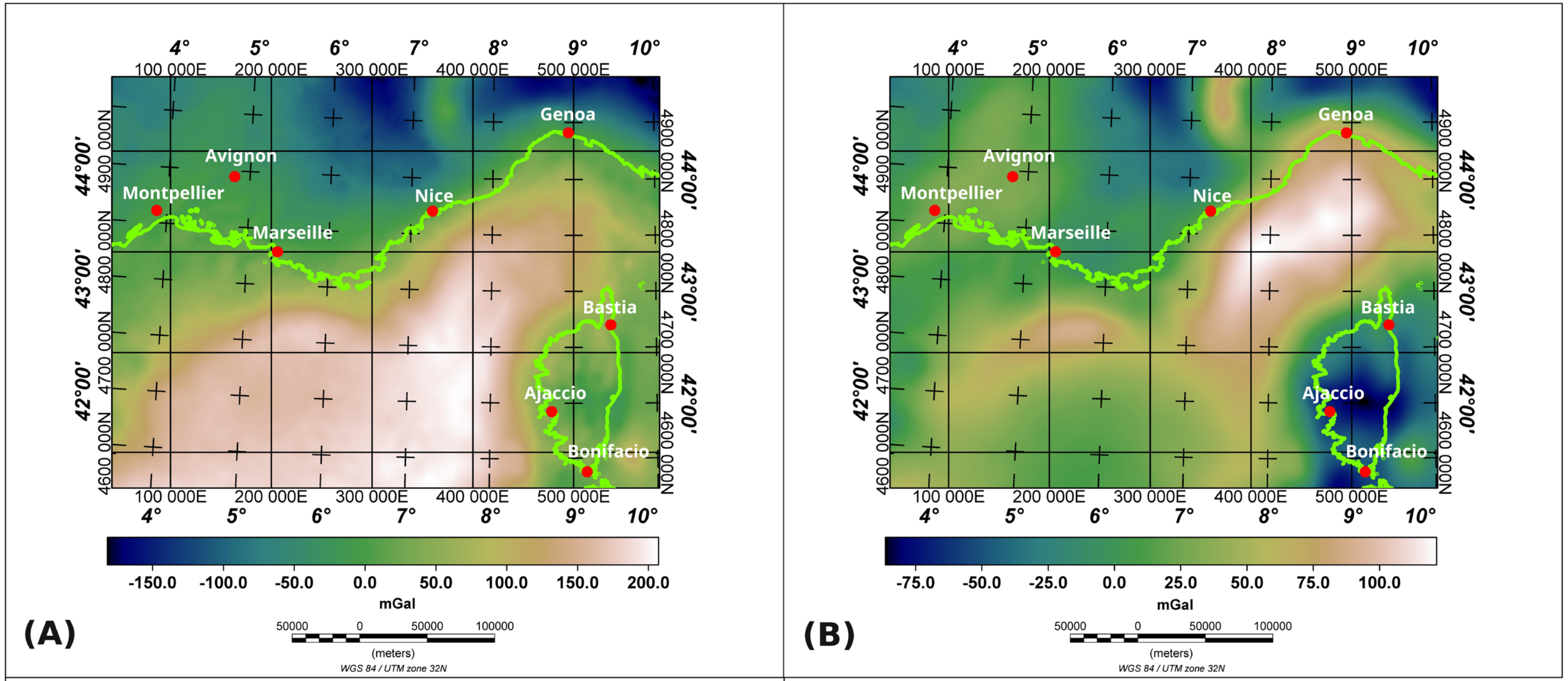

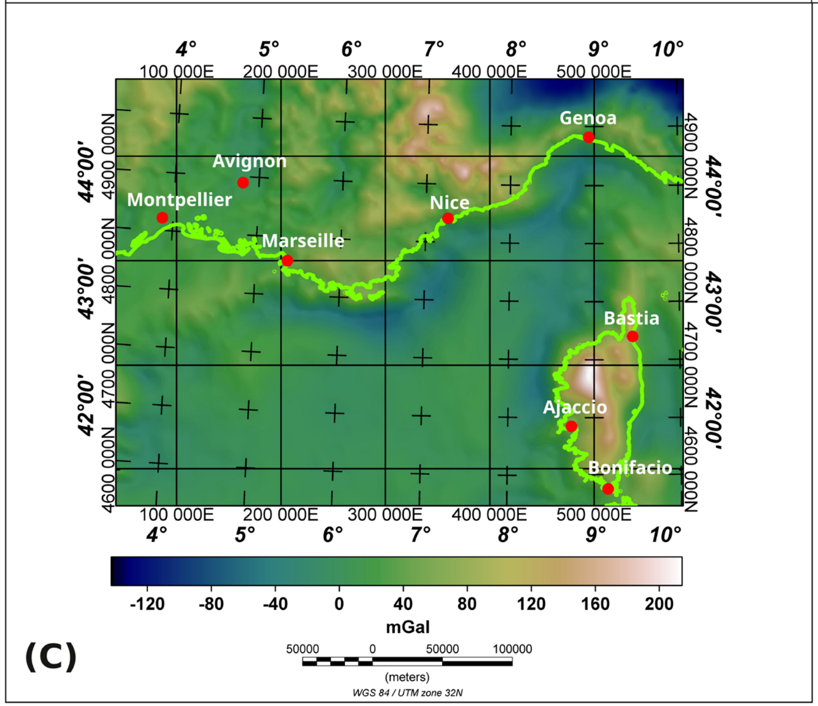

Gravity maps with the coasts marked with green lines. **(A)** Bouguer anomaly: The new AAGRG Bouguer gravity map of the Liguro-Provençal Basin. This map is based on a 4 km x 4 km grid of the complete CBA map. **(B)** The residual field of the CBA after elimination of regional anomalies that would hinder the interpretation in the local area of the Liguro-Provençal Basin.

(C) Free air anomaly: compiled by the AAGRG for the Alps and their foothills. On land, the Free air anomaly follows the topography of the surface. Offshore, in the Liguro-Provençal Basin, significant gravity differences can also be observed due to uneven bathymetry

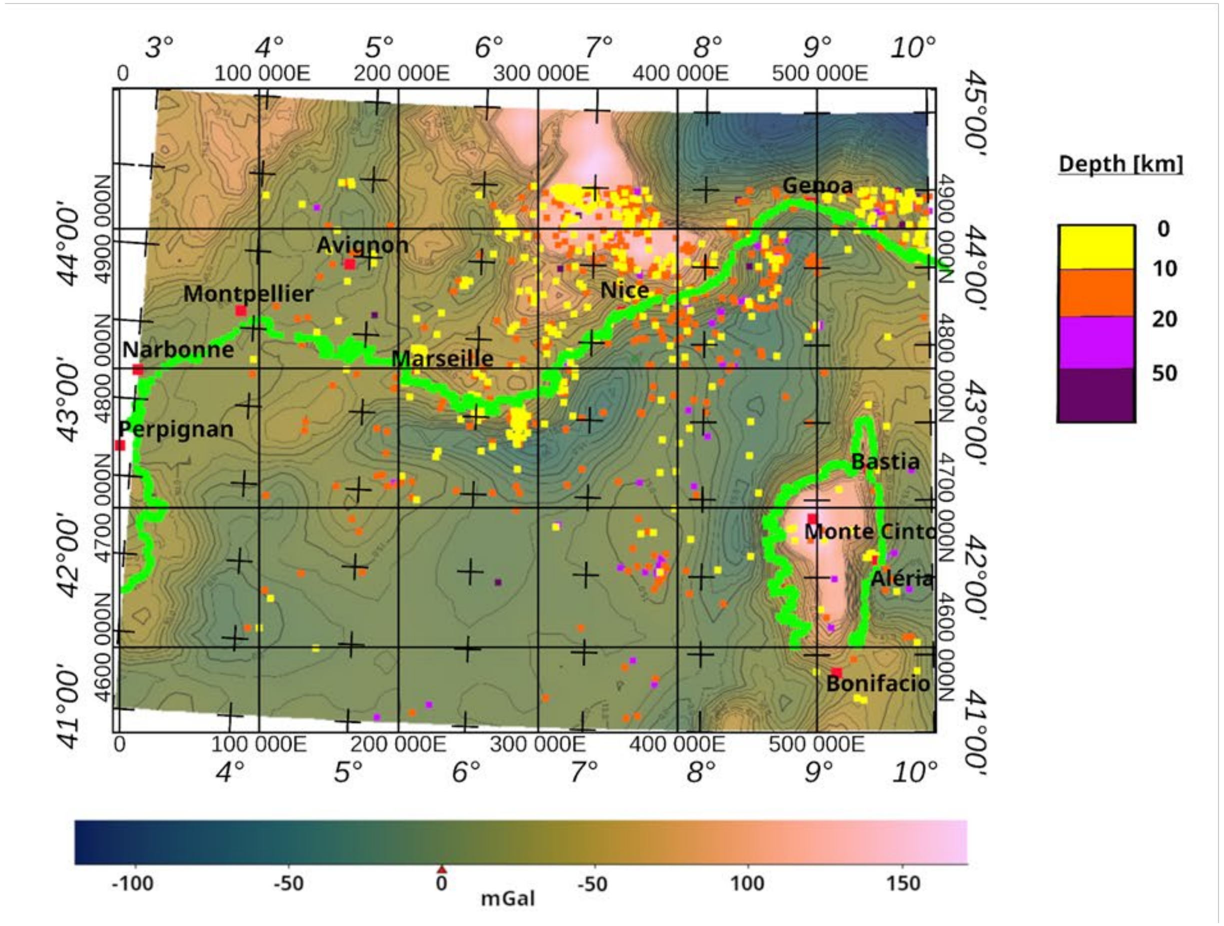

Distribution of earthquakes epi-centers with magnitude 2.5 and higher at depths between 0 and 100 km (NEIC 2021) and Free air anomaly.

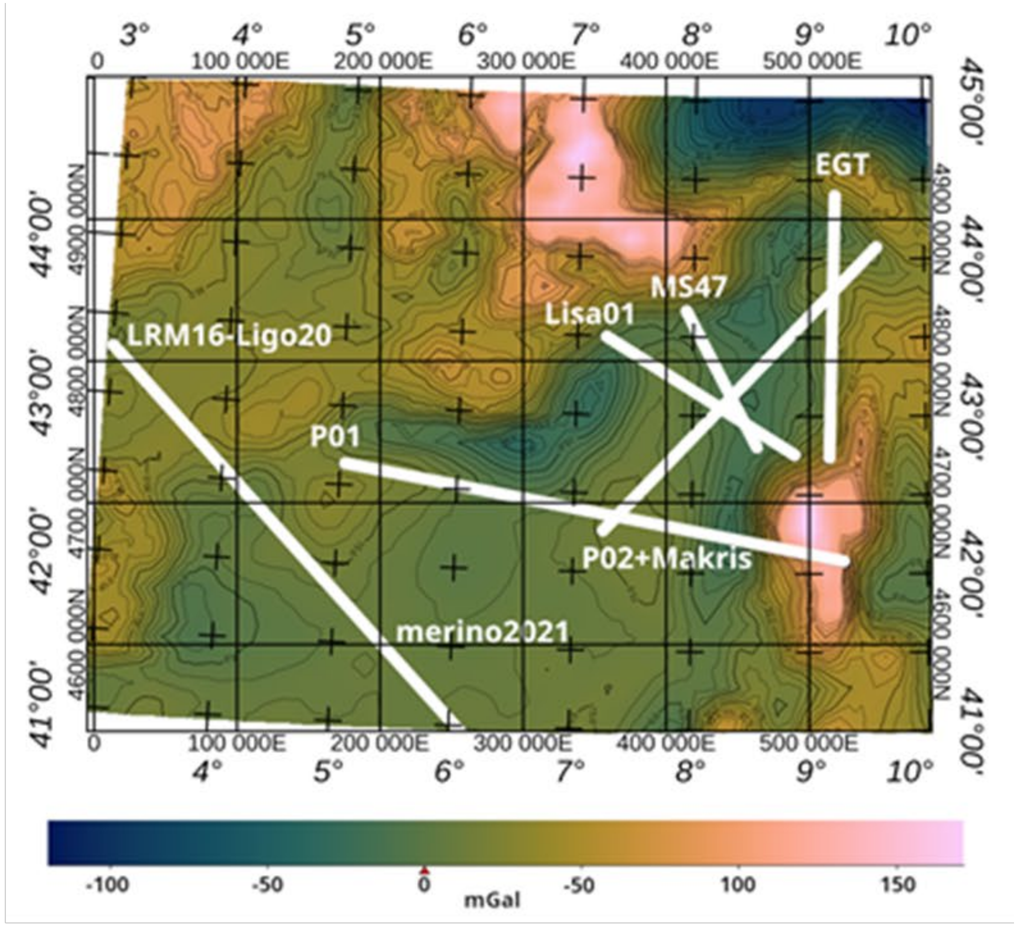

Location of the seismic profiles used to constrain the model and Free air anomaly.

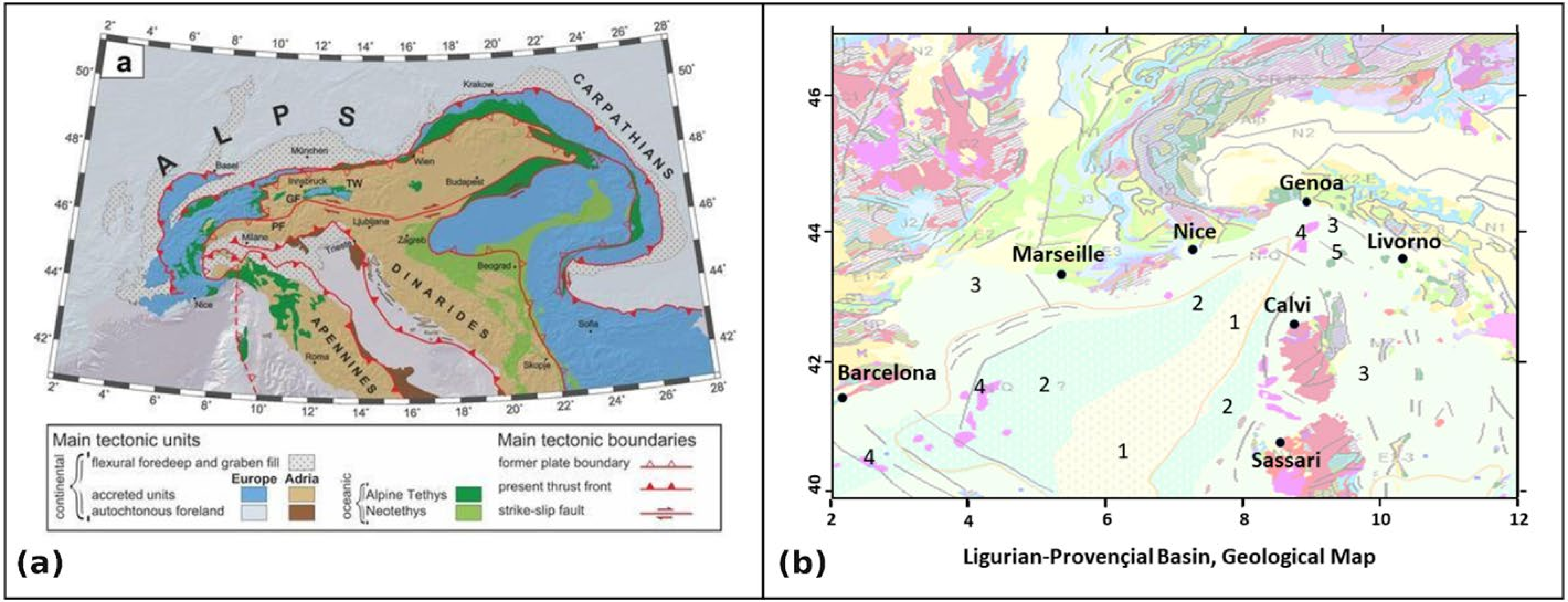

(a) Main Alpine tectonic units and **(b)** Submarine geological units (IGME 5000, after Asch (2003)): **1** oceanic crust formed during rifting in the area; **2** thinned continental crust stretched during rifting; **3** undifferentiated continental crust; spots in **4** are intrusions of igneous rocks; **5** represents ophiolites.

Methods used

Shape curvature

Roberts, A. (2001), Curvature attributes and their application to 3D interpreted horizons. First Break, 19: 85-100. https://doi.org/10.1046/j.0263-5046.2001.00142.x

Terracing and clustering

Cooper, G. R. J. (2020). An improved terracing algorithm for potential-field data. Geophysics, 85 (5), G109–G113. doi: https://doi.org/10.1190/geo2019-0129.1

Euler deconvolution

Pašteka, R. (2006). The role of the interference polynomial in the Euler deconvolution algorithm. Bollettino di Geofisica Teorica ed Applicata, 47, 1-2, pp. 171-180. https://bgo.ogs.it/issues/2006-vol-47-1-2/role-interference-polynomial-euler-deconvolution-algorithm

3D gravity modeling IGMAS+

D. Anikiev, H.-J. Götze, C. Plonka, M. Scheck-Wenderoth, S. Schmidt (2023). IGMAS+: Interactive Gravity and Magnetic Application System (Version 1.4). GFZ Data Services. https://doi.org/10.5880/GFZ.4.5.igmas.v.1.4

Gravitational Potential Energy

Ghosh, A., Holt, W.E., and Flesch, L.M. (2009). Contribution of gravitational potential energy differences to the global stress field, *Geophysical Journal International*, Volume 179, Issue 2, Pages 787–812, https://doi.org/10.1111/j.1365-246X.2009.04326.x

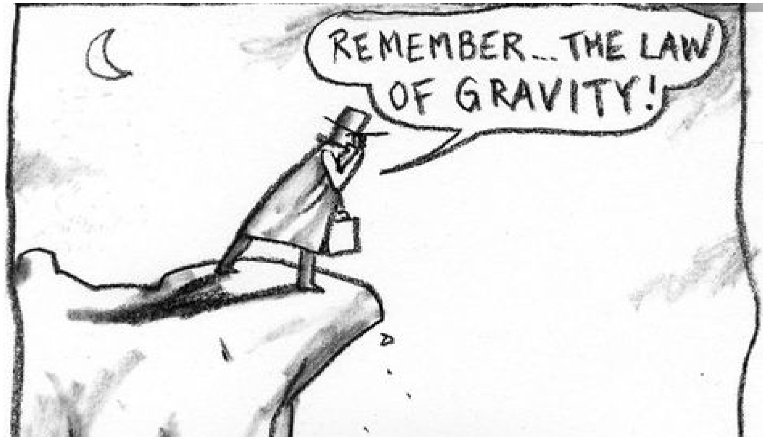

Results & interpretation

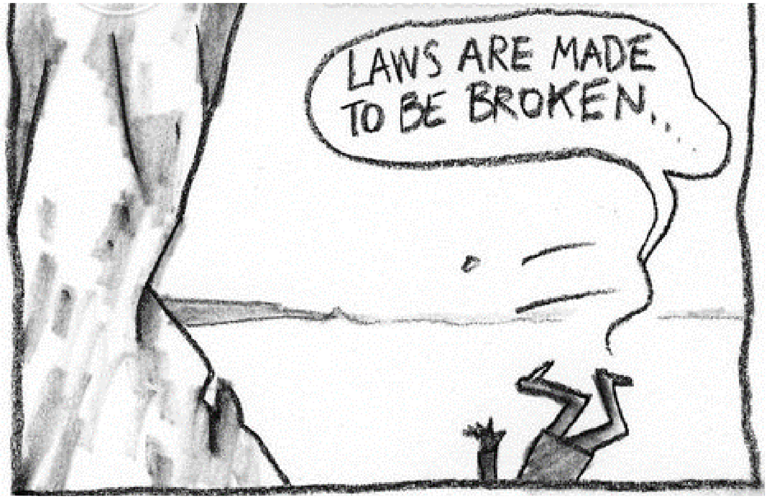

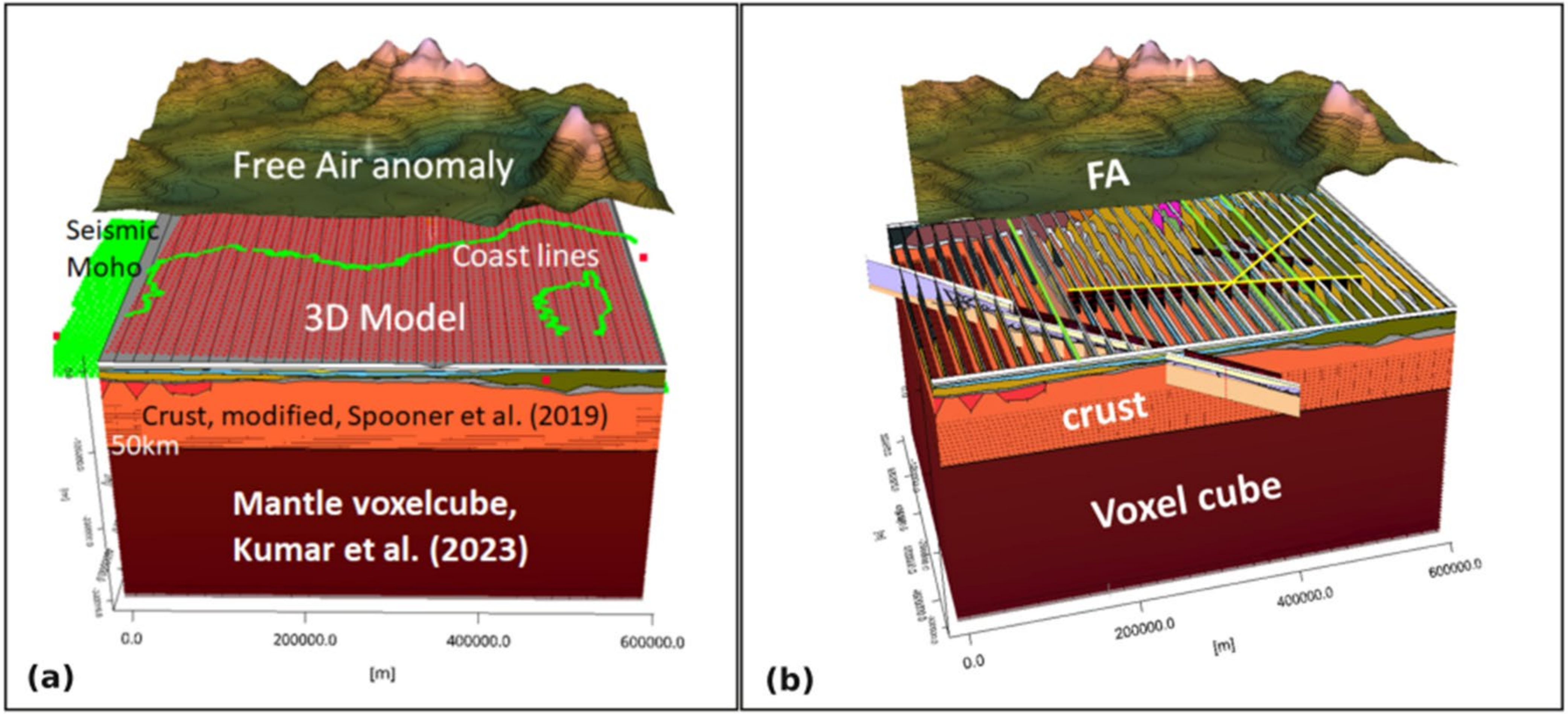

The **3D model looking North with Free air anomalies** above the actual model (a) and (b). Below, on the pink layer, one can see both the vertical sections on which the 3D model is defined, and the positions of the approximately 3000 model stations (pink dots) which are removed in (b). In green: seismic Grad-Moho (Grad et al., 2012), loaded for comparison purposes. Below is a view of the model crust with different crustal structures (different colors, table above) down to a depth of 50 km. The mantle voxel cube (dark brown) contains the upper mantle velocities converted to densities according to Kumar et al. (2022).

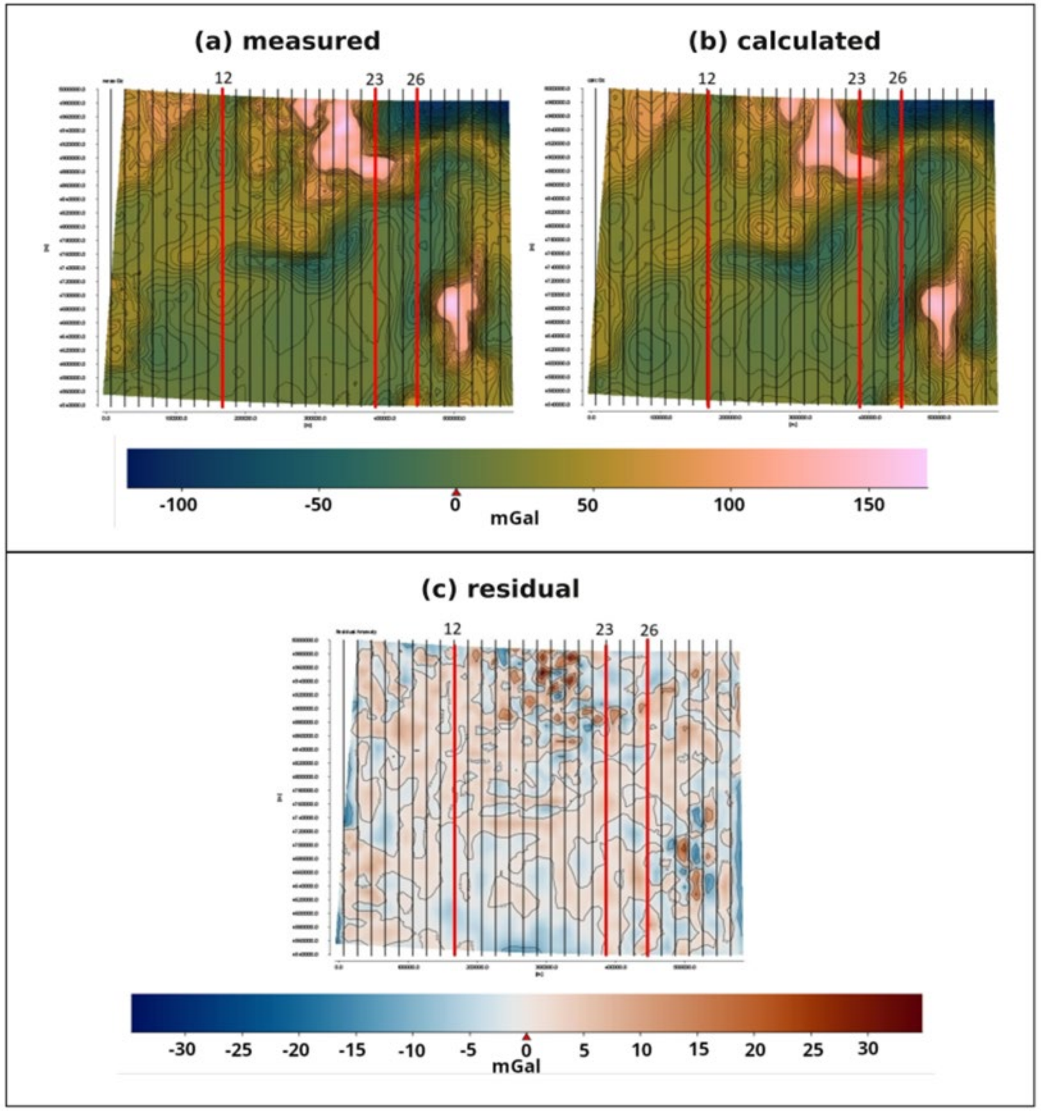

The **resulting gravity maps** of the Liguro-Provençal Basin modelling: upper panel from left to right: (A) **Free air anomaly** - (B) **calculated model gravity**; lower panel (C) - **residual field** of both.

Name	Density[kg/m³]
01_Water	1024.999998
020_Loose_Sed	2200.0
021_Loose_Sed_Molasse	2200.0
022_Loose_Sed_Po	2200.0
030_Con_Sed	2400.0
031_Con_Sed_Molasse	2400.0
032_Con_Sed_Po	2698.198993
04_U_Crust_Apennine	2720.0
05_U_Crust_Distant_Dense	2720.0
06_U_Crust_Moldanubia	2699.999998
07_U_Crust_Bohemia	2740.0
08_U_Crust_North_east	2679.999999
09_U_Crust_Saxothuringia	2700.0
10_U_Crust_Vosges	2659.999998
11_U_Crust_Molasse	2720.0
12_U_Crust_E_Alps	2739.999999
13_U_Crust_nae_Clue	2730.0
14_U_Crust_W_Alps	2700.0
15_U_Crust_Po	2700.0
16_U_Crust_NE_Adria	2629.999984
17_U_Crust_Ivrea	2700.0
18_U_Crust_SE_Adria	2699.999999
19_L_Crust_North_West	2761.379007
20_L_Crust_North	2917.336256
21_L_Crust_Europe	2789.616911
22_L_Crust_North_East	3106.348911
23_L_Crust_West	2960.0
24_L_Crust_E_Alps	2946.746194
25_L_Crust_East	3049.999995
26_L_Crust_Ivrea	3103.011971
27_L_Crust_Liguria_and_Apennine	2820.0
28_L_Crust_Adria_and_Corsica	3032.036036
29_Mantle	3506.580529
30_Mantle_2	3406.657679
31_Base	3314.999991
Top	0.0
reference	0.0

Table: **Model densities** used in our model of the Ligurian Liguro-Provençal Basin. (after Spooner, 2019). Note: Density values with 6 decimal places are *calculated by inversion.*

P01

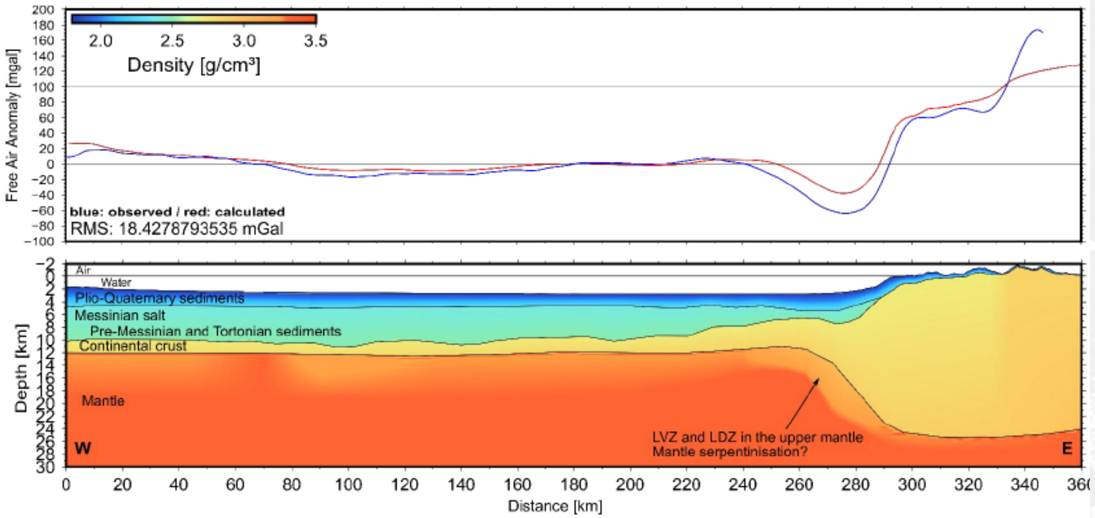

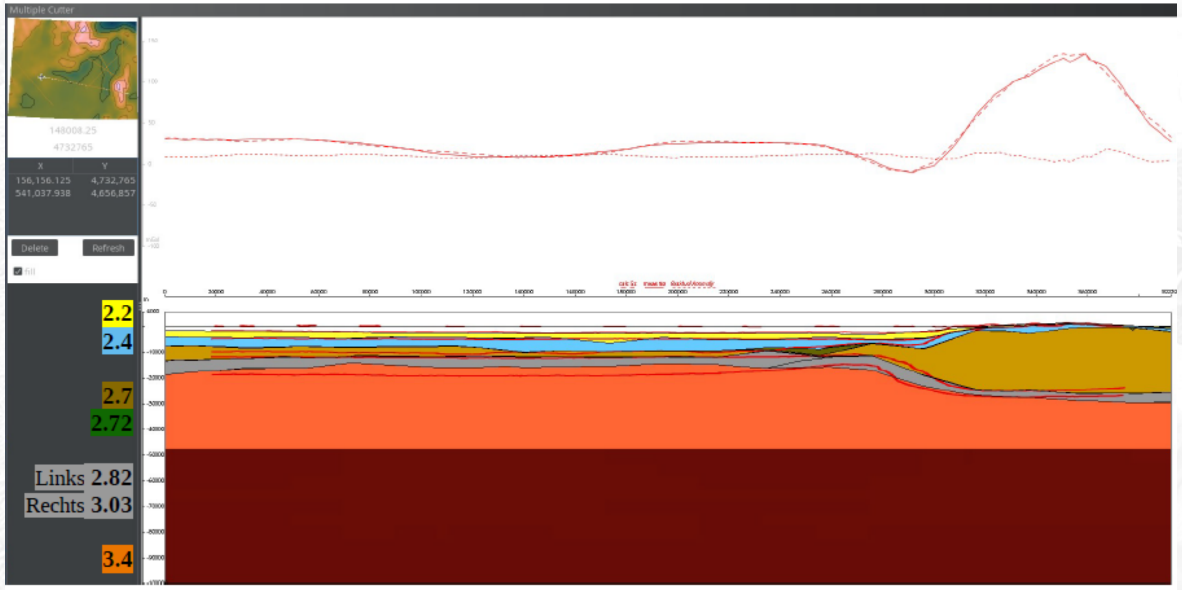

P02+Makris

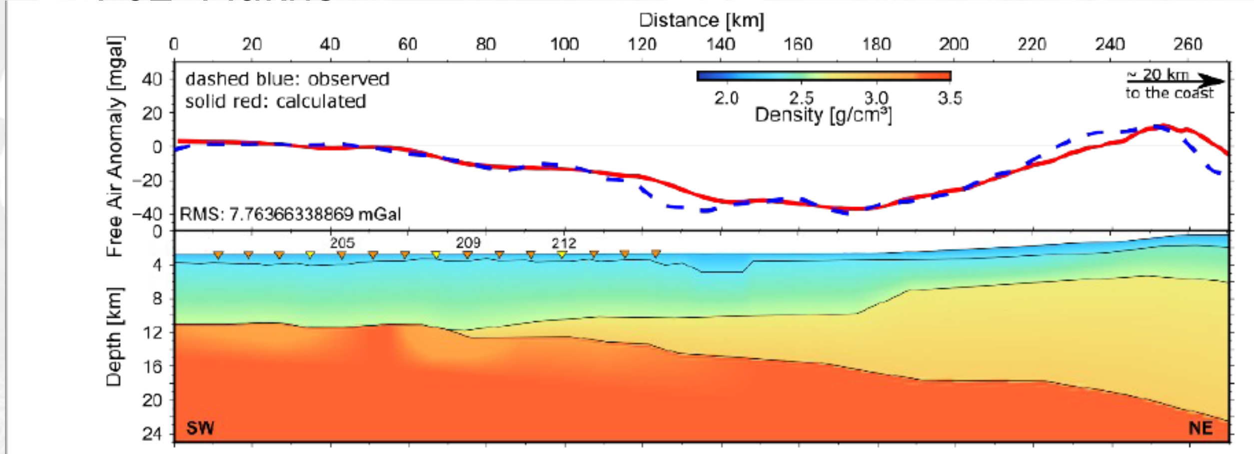

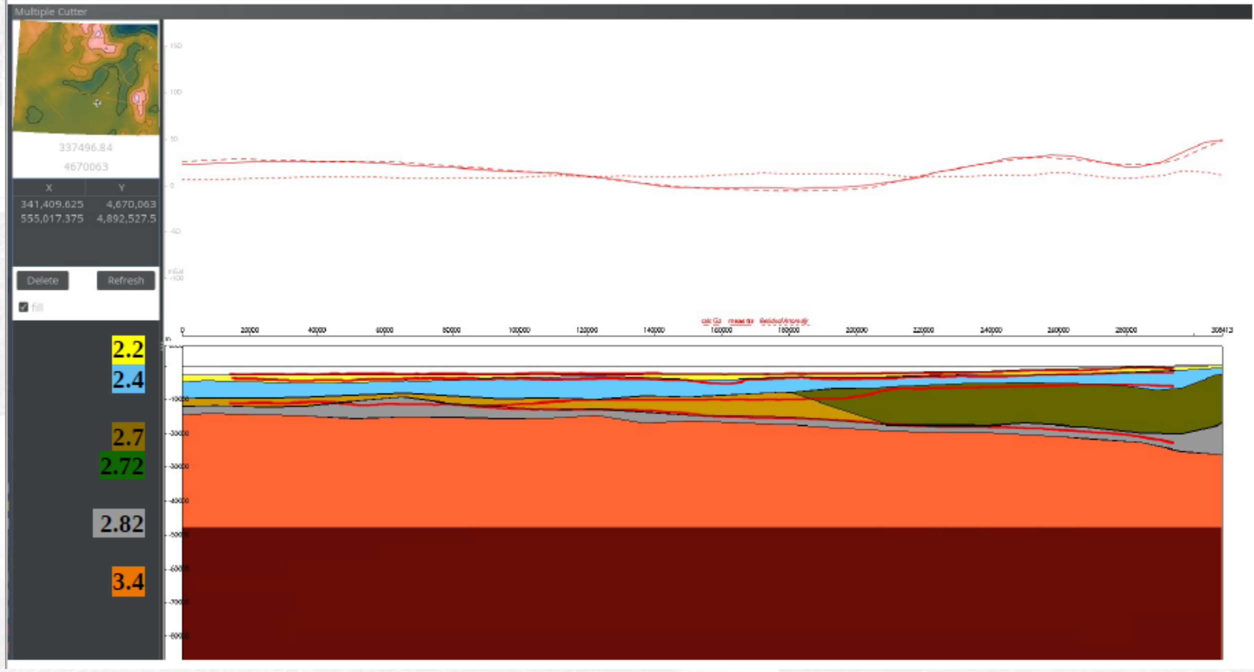

Model constraints:

GEOMAR reflection/refraction seismic studies (LOBSTER, Anke Dannowski) & 2D density model, along profiles P01 & P02+Makris (upper series). IGMAS modelling, lower series)

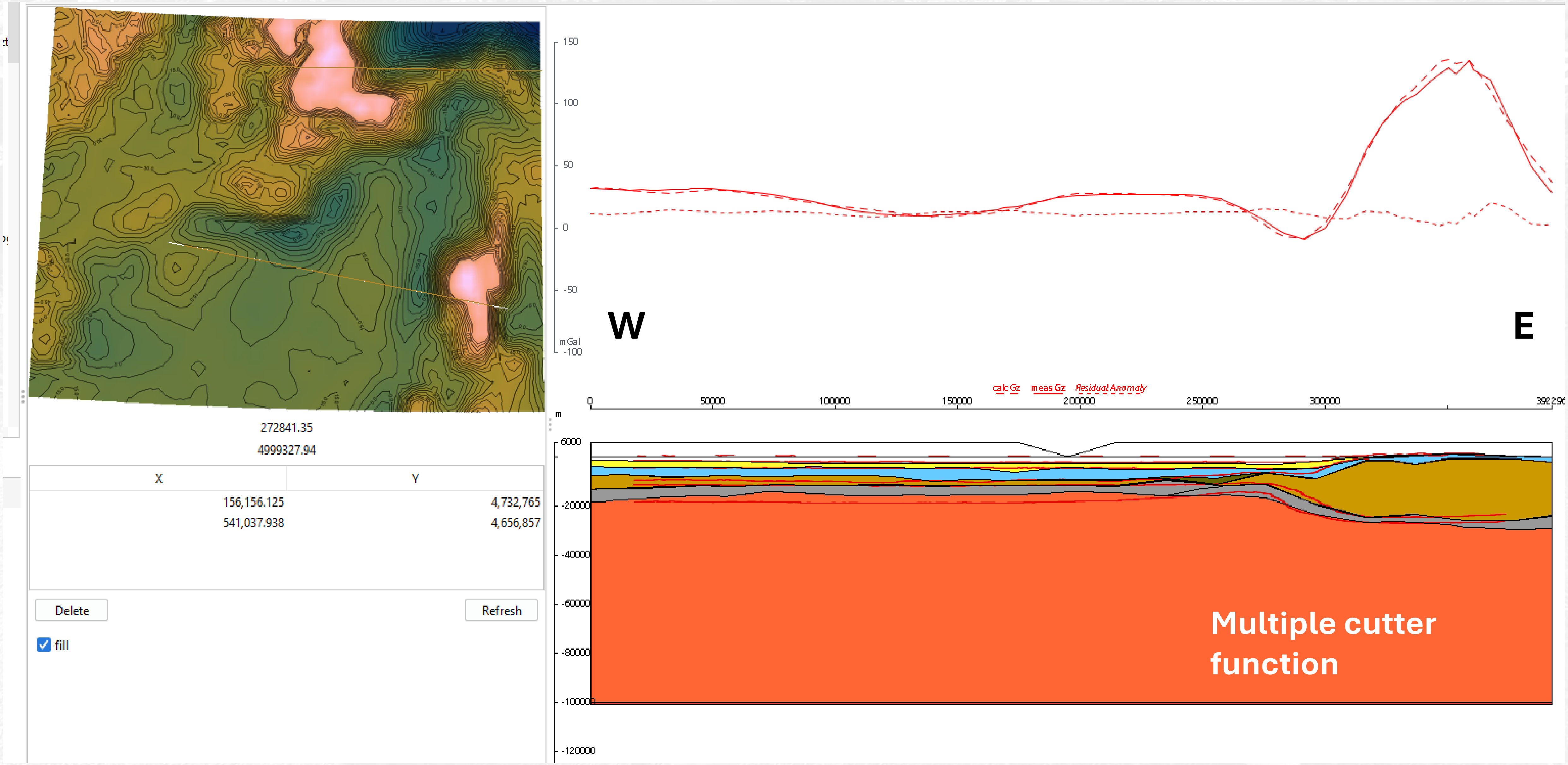

IGMAS screenshot: Profile „LOBSTER P01“ (left/W: French coast – right/E: Isle of Corsica)

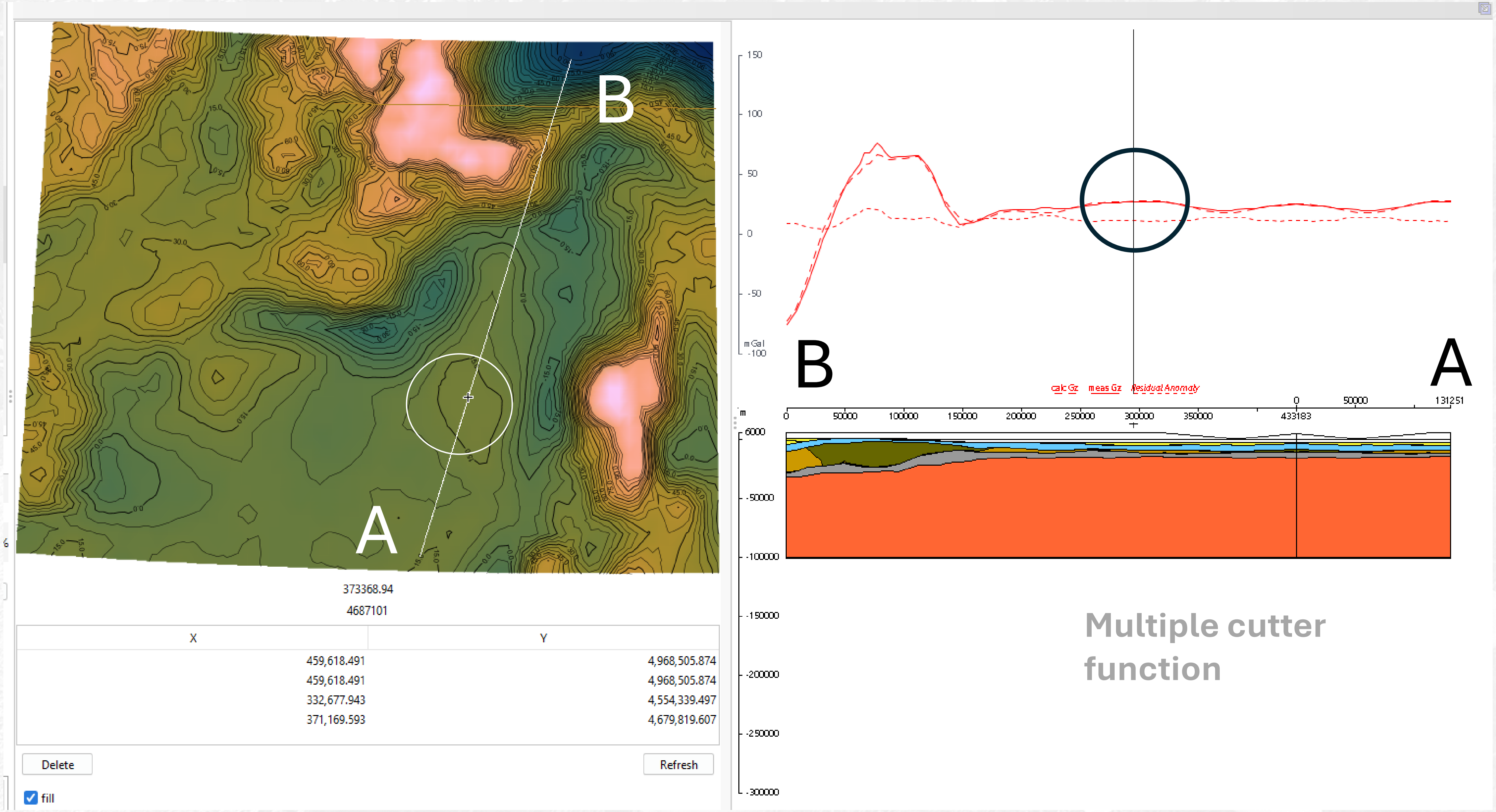

IGMAS screenshot: Profile along the axis of measured central gravity „high“ (B = Southern Alps/Apenin)

Map view of the actual 3D Model (including the modified crustal „Cameron model“ - polyhedrons) with the voxelcube of the „dynamic_model“ between the depths of 50 – 300 km (grey)

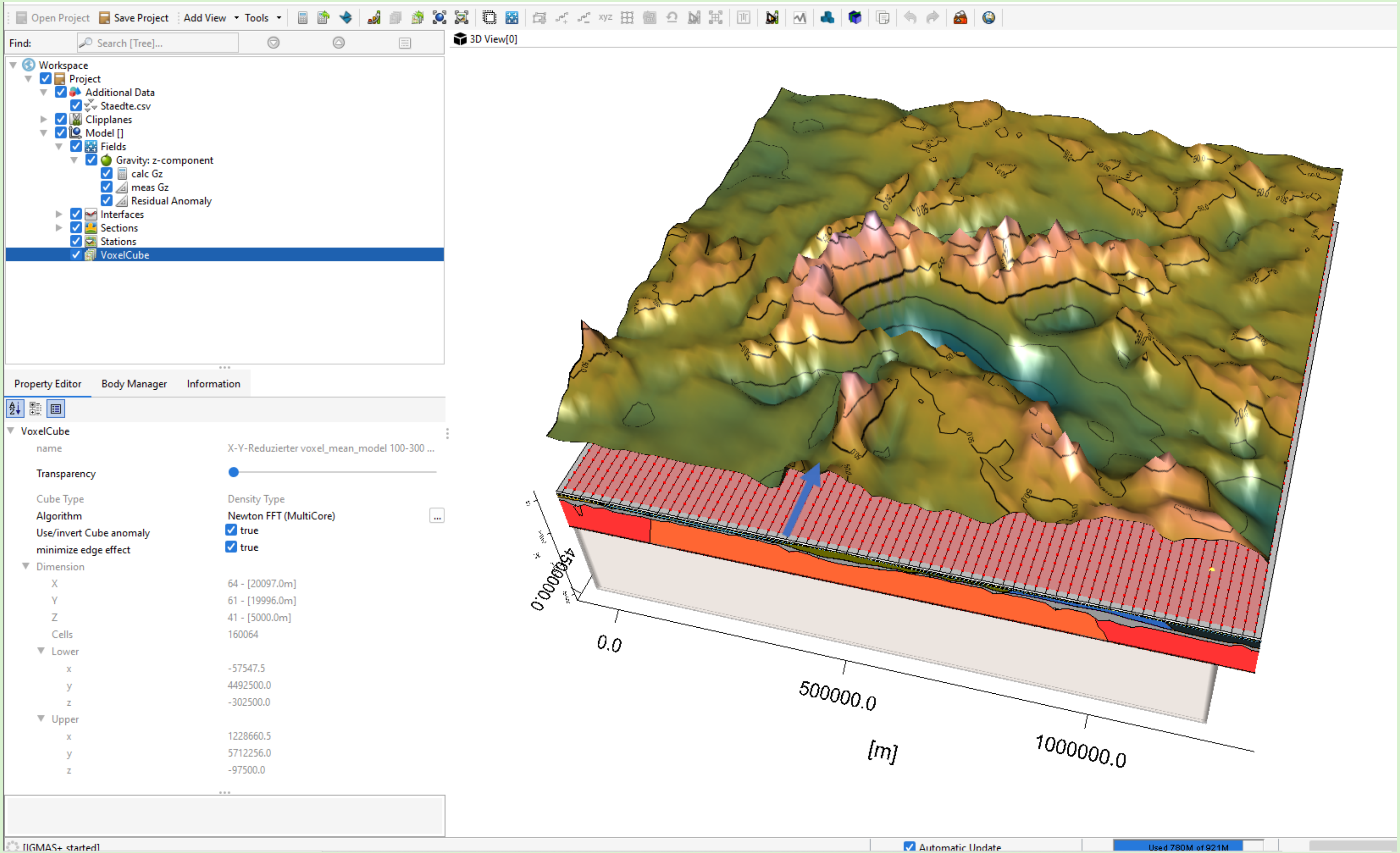

3D view of the gravity effect of the voxelcube „dynamic_model“,

depths between 50 – 300 km

$\Delta_{max\text{-}min}$ ~ 140 mGal

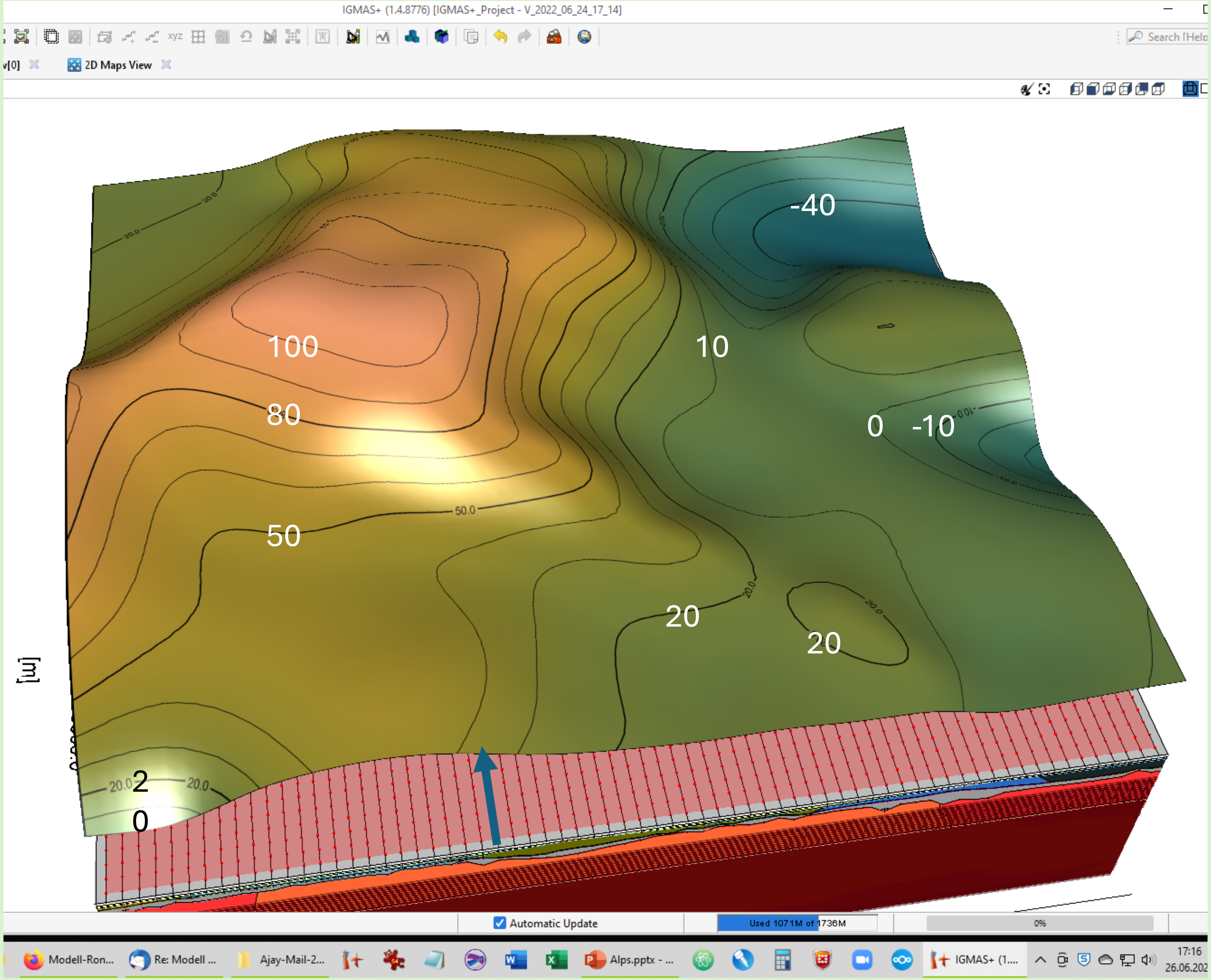

Section 25, gravity effect of the voxelcube „dynamic model“, depths between 50 -300 km, in relation to the measured field (Free Air anomaly)

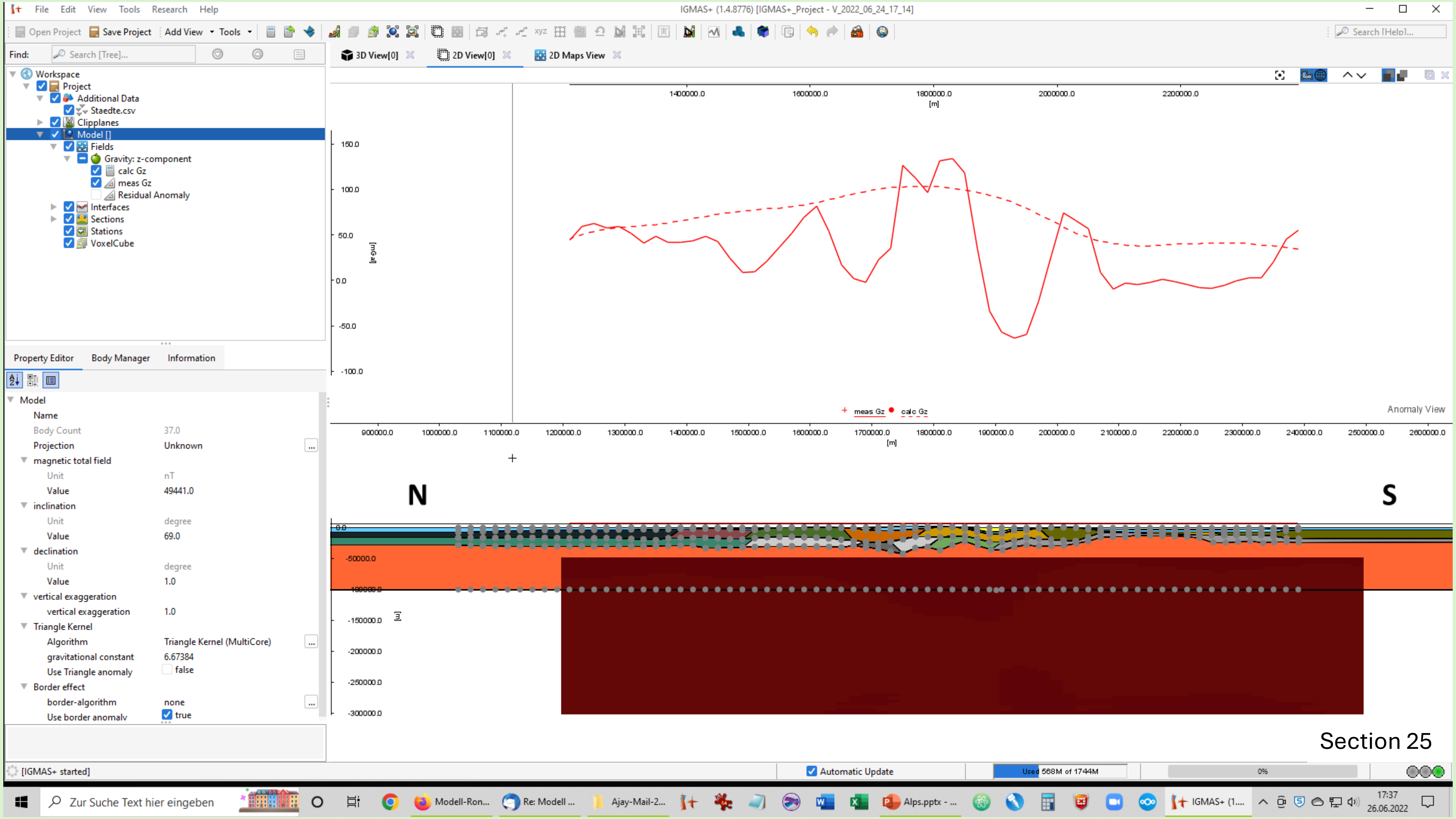

Cross section 25, 3D Model (based on a modified crustal „Cameron model“) with the voxelcube „dynamic model“ between the depths of 50 – 300 km

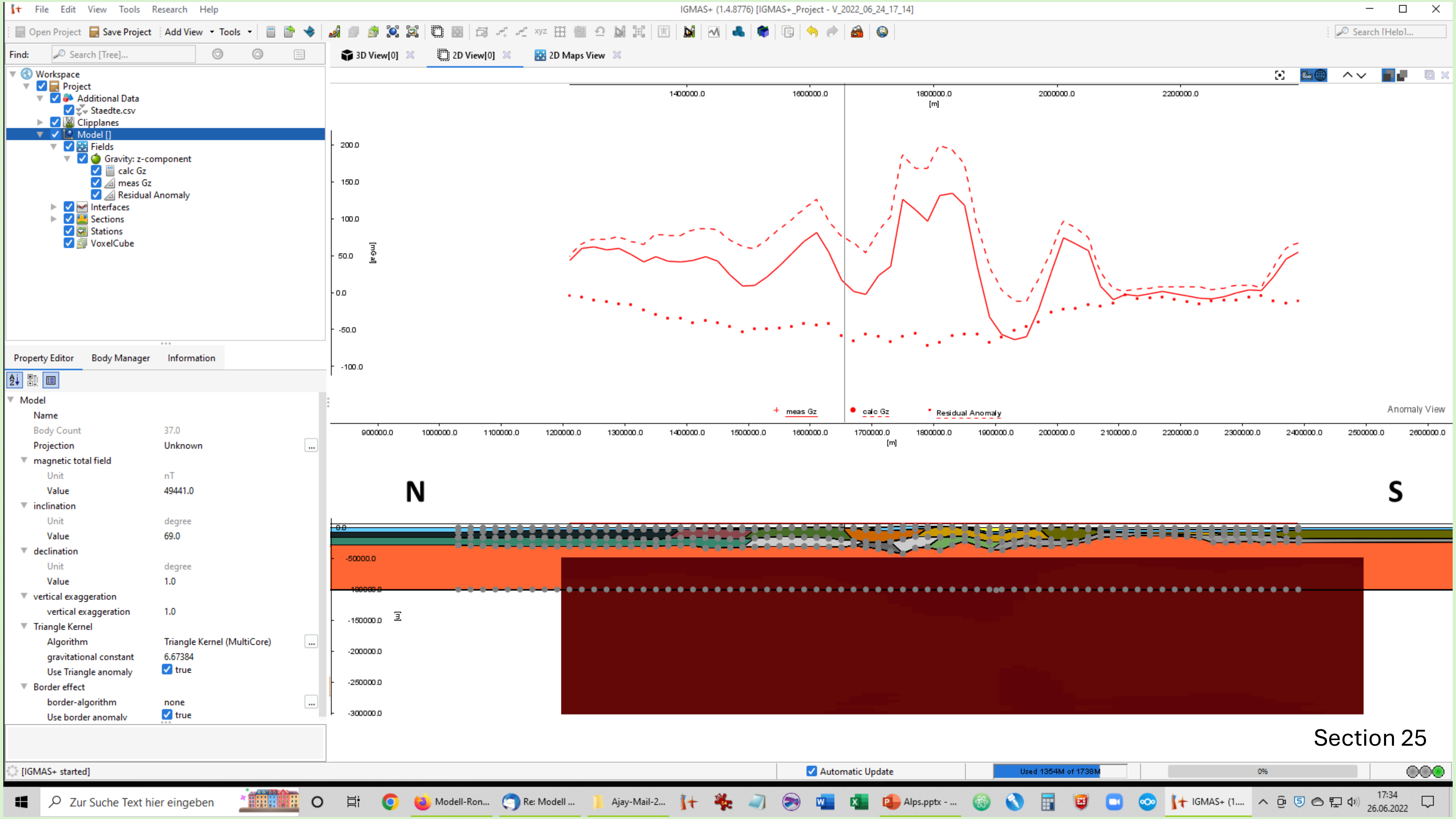

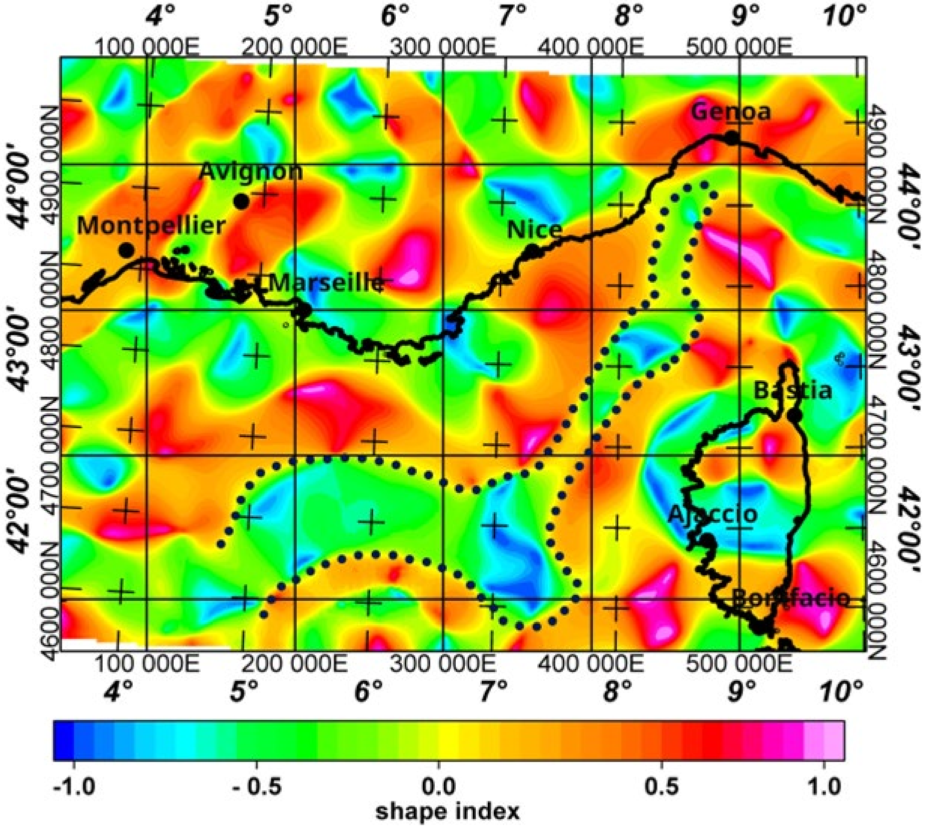

Shape curvature calculation of the residual field. The **red** tones visualize "**ridge-like**" structures by a rather high shape index, on which some local **maxima of shape index** lie (magenta). The blue-green shades indicate areas of lower shape index ("**valleys" or "lows**" as mentioned by Roberts, 2001).

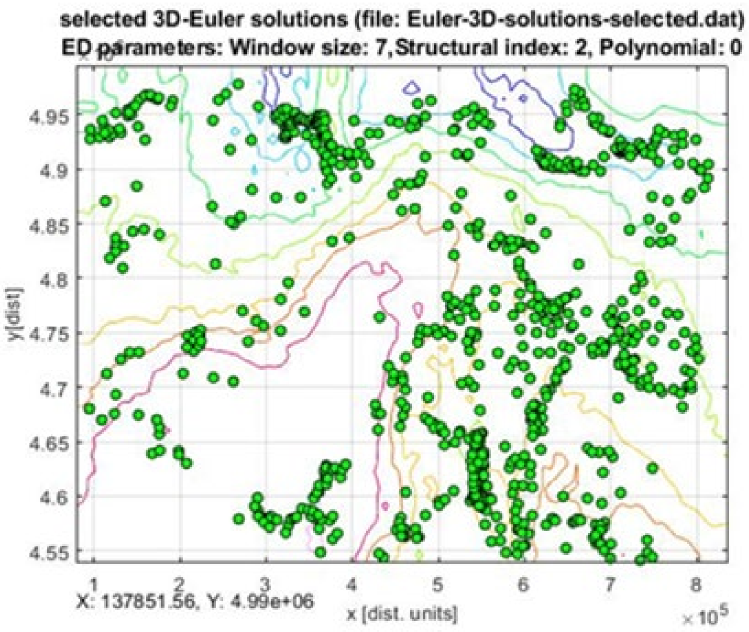

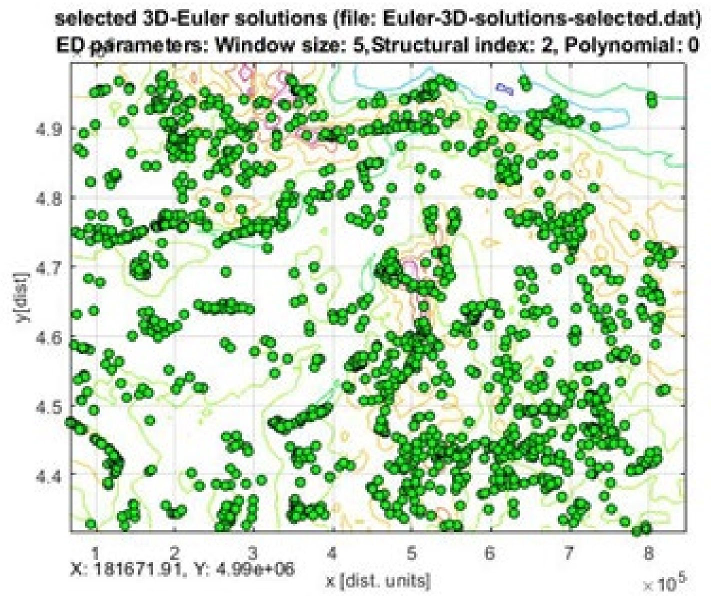

EULER DECONVOLUTION: For the Bouguer anomaly analysis (left) we selected a window size (WS = 7) units, for the Free Air (right) WS = 5. The structure index is set to 2 for both fields, which refers to a three-dimensional source.

(A) Positive gravitational potential energy (GPE) typically indicates areas where the crust is thicker or denser. This suggests regions where compressional stress is dominant, leading to crustal thickening or uplift.

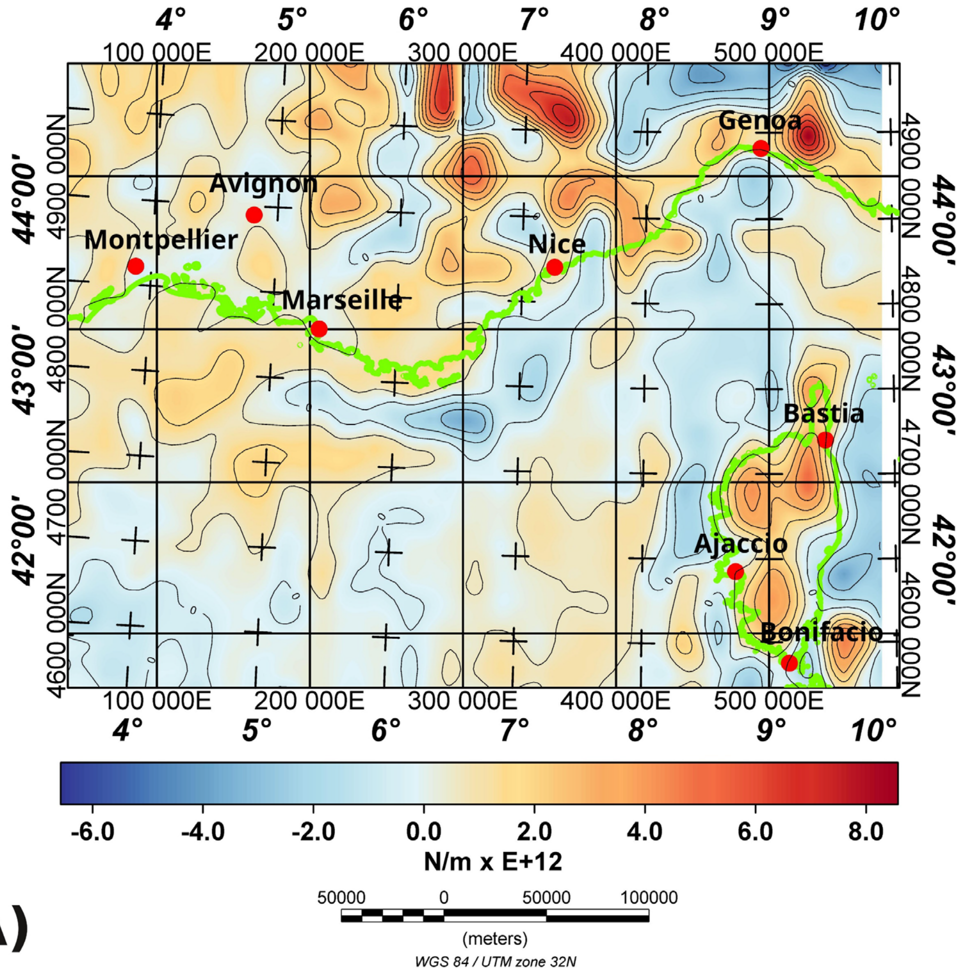

(A)

(B) Vertical stress (ZZ) distribution shows that areas with positive GPE are likely to experience higher vertical stress due to compression, while areas with negative GPE may have lower vertical stress due to extensional forces

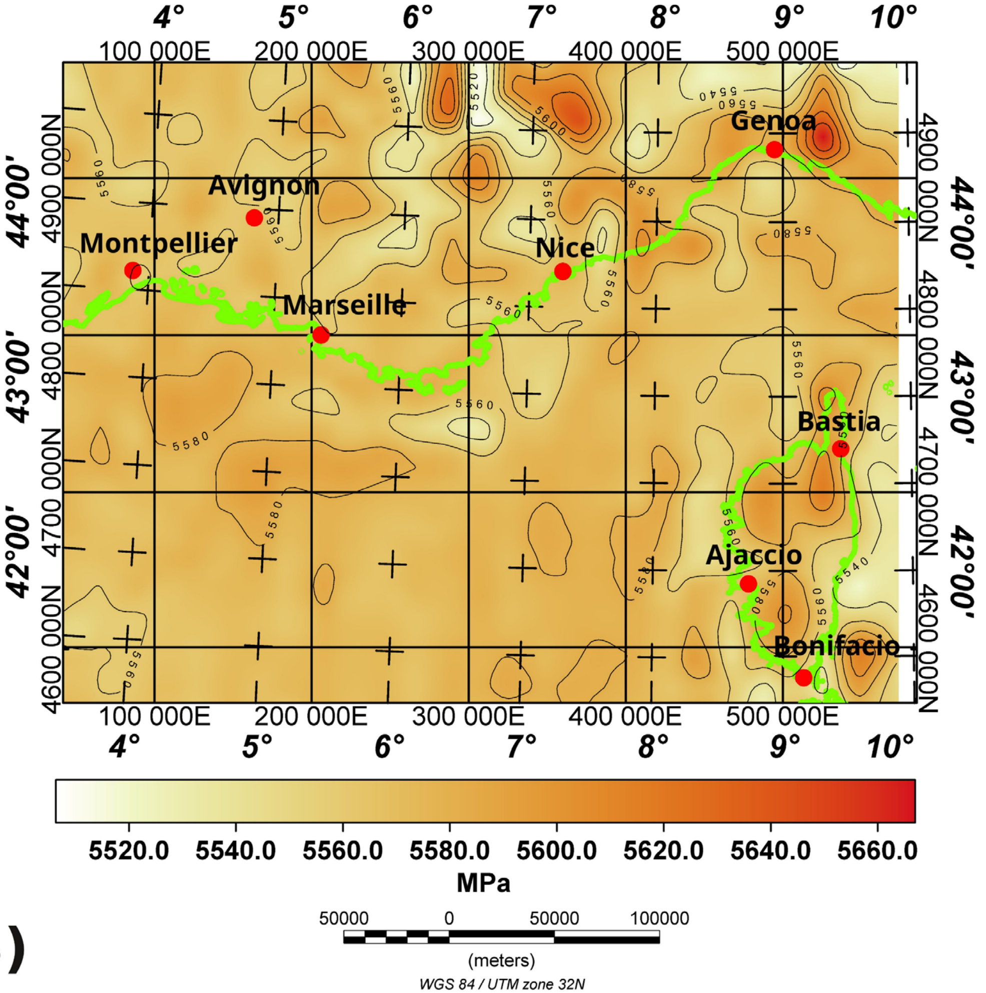

(B)

BA Terracing

&

BA Clustering

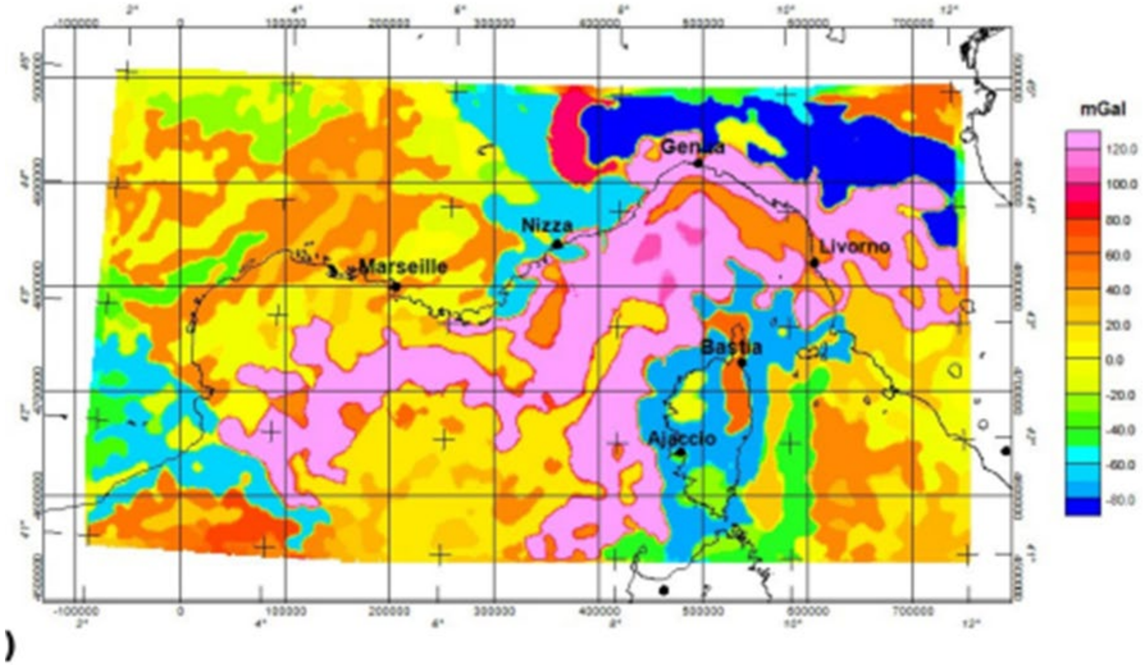

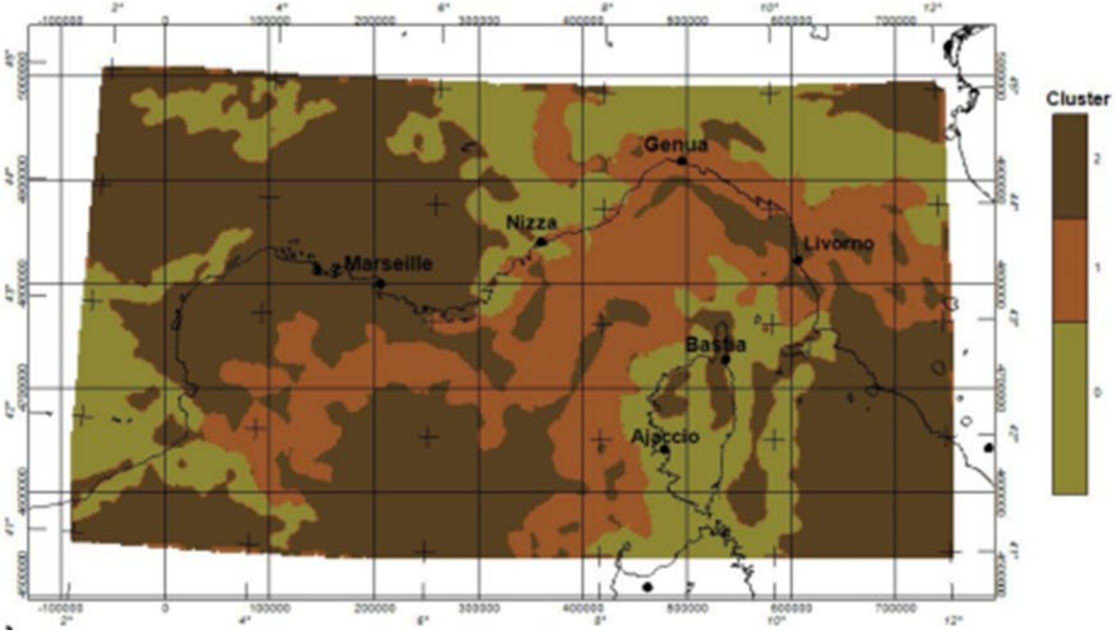

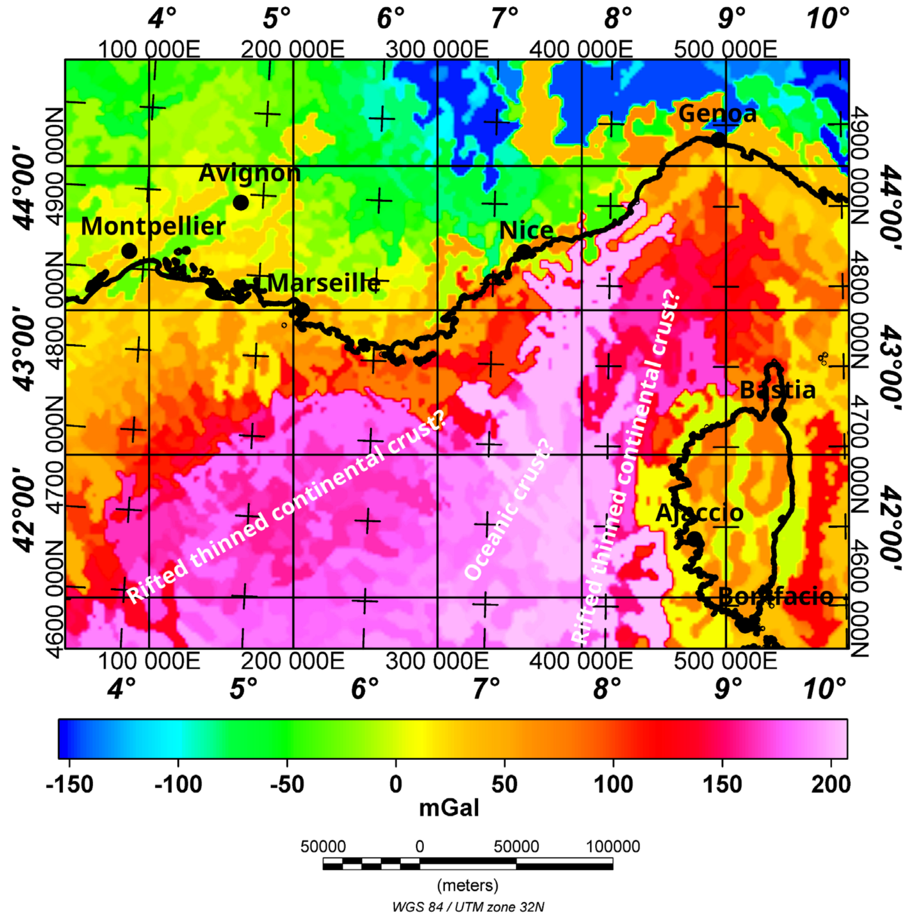

Terracing was calculated with minimum curvature, grid spacing of 2 km, a gamma threshold of 0.1 and 200 iterations; (residual gravity field).

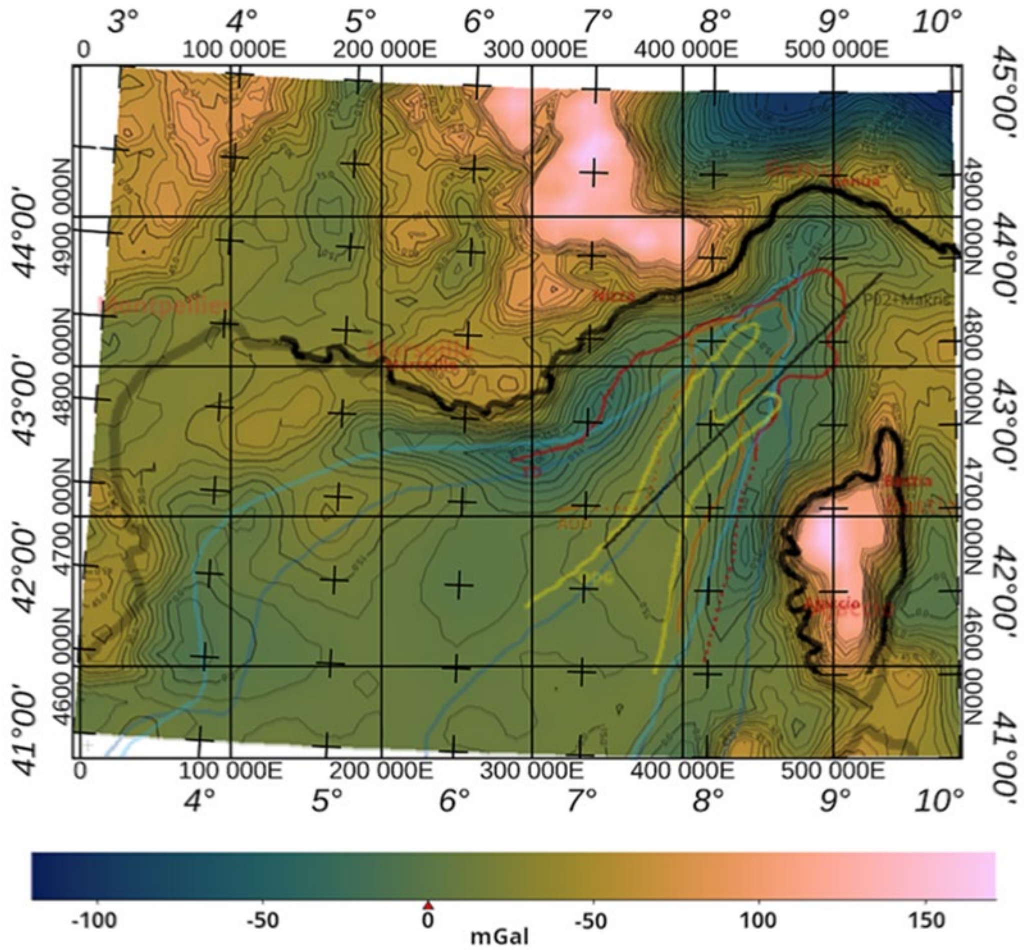

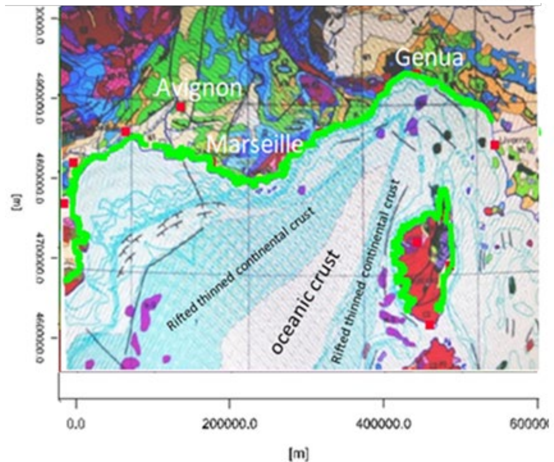

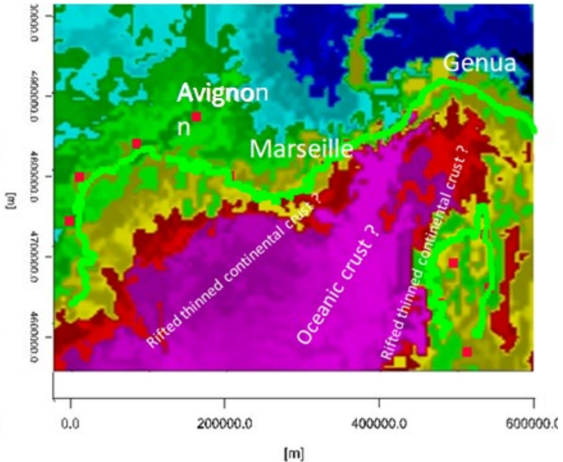

Visual correlation of proposed areas of different crustal types: The boundaries of the different domains from the work of:

- Asch (2003) in blue color and the work of
- Dannowski et al. (2020) and
- Rollet et al. 2002) (yellow and red lines)

of **free gravit**y were superimposed.

The overlay shows that the main contours of the central gravity high coincide well with independently proposed crustal domains. The black line in the center indicates the position of the P02+Makris seismic profile.

Left: **Geological map** of Asch (2003) (left) and the **terraced Bouguer anomaly** (right).

Evidence for rifting of the basin from data and methods used

Observation/analysis results for rifting processes	YES	NO
AAGRG and smoothed Free air anomaly (chapter 3.3)	**X**	
AAGRG and smoothed Bouguer anomaly, residual gravity (chapter 3.2)	X	
Terracing & Clustering results (chapter 5.2)	**X**	
Shape curvature (chapter 5.1)	**X**	
3D-modeling (chapter 5.3)	X	
Euler deconvolution (chapter 5.5. and appendix)		x
Gravitational potential energy (chapter 5.4)	X	
Combined interpretation (chapter 6)	X	

X = strong indication
X = unclear/ambiguous
x = weak indication

Acknowledgements:

The authors acknowledge funding from the *Deutsche Forschungsgemeinschaft (DFG)* through the project (DEFORM)" within the SPP 2017. We would like to acknowledge the pleasant collaboration with our *colleagues in the AlpArray Gravity Research Group (AAGRG) and the SPP 2017 (MB4D)*. We are very grateful to the IGMAS+ Team and particular to *Dr. Cameron Spooner* for his first compilation of the 3D Alpine density model (PhD thesis), *Dr. Ajay Kumar* for calculating the density voxel cube and to *Dr. Judith Bott* for her permanent interest and valuable hints regarding density modeling.

IGMAS+ Website: https://www.gfz-potsdam.de/igmas

MB 4D Mountain Building Processes in 4D

ALP ARRAY

DFG Deutsche Forschungsgemeinschaft German Research Foundation

CAU Kiel University Christian-Albrechts-Universität zu Kiel

GEOMAR Helmholtz Centre for Ocean Research Kiel

GFZ Helmholtz-Zentrum Potsdam